AIMS Mathematics, 11(3): 7821–7844.
DOI: 10.3934/math.2026322
Received: 07 January 2026
Revised: 06 March 2026
Accepted: 11 March 2026
Published: 24 March 2026

https://www.aimspress.com/journal/Math

Research article

Dynamic event-triggered approach for practical fixed-time cluster synchronization control of multilayer complex networks under denial-of-service attacks

Ling Liu*

School of Mathematics and Systems Science, Guangdong Polytechnic Normal University, Guangzhou 510000, China

* **Correspondence:** Email: Lgliu0@163.com.

Abstract: This paper is concerned with the practical fixed-time cluster synchronization control problem of a class of multilayer complex networks (MCNs) with different nonlinearly coupled nodes in different layers under denial of service (DoS) attacks. Each node in the MCNs is modeled by a nonlinear dynamic system. The central aim is to make the error between each cluster of nodes to its own reference trajectory converge to a bounded region in fixed time, while simultaneously achieving communication efficiency for each node. Toward this aim, a distributed dynamic event-triggered mechanism resilient to DoS attacks is proposed such that each node can make its own decisions to transmit (or not) its data of interest over the communication channel. Second, by suitably modeling the DoS attacks, event-based cluster synchronization controllers are constructed that incorporate the dual effects via two core design strategies: Setting the control input to zero during the active DoS attack intervals and adopting a zero-order hold strategy to keep the control input constant with the latest transmitted state data during the inter event intervals of the event-triggered mechanism. Sufficient conditions ensuring the practical fixed-time cluster synchronization of the MCNs under DoS attacks are established by constructing some appropriate Lyapunov functionals. Finally, an illustrative example is presented to validate the effectiveness of the main theoretical results.

Keywords: multilayer complex networks; cluster synchronization; practical fixed-time; DoS attacks; event-triggered control; nonlinear couplings; cyber-physical security
Mathematics Subject Classification: 37M05, 37M25

1. Introduction

Complex dynamic networks (CDNs) which can be modeled as a large number of nodes described as linear or nonlinear dynamic systems have attracted considerable attention from researchers due to

their wider applications, from smart grids to control of the transportation network. Many studies about dynamic characteristics of CDNs have been reported [1, 2]. It is worth mentioning that the coupling form and the dynamics between different nodes are usually different in real-world networks; for example, the brain network has intricate links and social networks have various media apps. However, traditional single-layer networks usually assume homogeneous coupling structures. Thus, it is important to research the dynamics of heterogeneous multilayer complex networks (MCNs) to improve our ability to understand and analyze actual networks [3, 4].

Synchronization, as one of the most important collective dynamic behaviors of dynamic systems, has been investigated by scientists for decades, including complete synchronization [5], phase synchronization [6], and lag synchronization [7]. Authors in [8] studied the quasi-synchronization issue for variable-order fractional complex dynamical networks and [9] investigated the intermittent synchronization issue for multiple moving agents. Several classes of synchronization conditions have been published, such as the master stability function method [10], the matrix measure analysis method [11], and the Lyapunov function method [12]. Moreover, there have been numerous studies on interlayer synchronization and intralayer synchronization for MCNs [13, 14]. Due to the fact that nodes in actual networks are required to present the various functions to complete multi object tasks effectively, this means hat nodes distributed in the same or the different layers will show different dynamic properties. Such a phenomenon cannot be described as complete, interlayer, or intralayer synchronization for the sake of brevity. However, cluster synchronization (CS) can accurately simulate it. In fact, CS is more often observed in nature than the others, such as wolves hunting, neurons discharging in the brain, and multi-objective rescues. A number of researchers are dedicated to studying CS issues for single-layer complex dynamic networks and multilayer complex dynamic networks [15, 16].

On the other hand, the convergence speed of states is an important indicator for evaluating the effectiveness of control design schemes for dynamic systems, especially for engineering processes with high precision requirements. Actually, systems achieving an ideal state in infinite time is unrealistic. Taking this into consideration, scholars analyze the finite-time control issues to ensure the systems reach the goal within a specific time -frame [17, 18]. Furthermore, Polyakov proposed the fixed-time control strategy [19], compensating for the deficiency of convergence speed related to the initial conditions and providing a faster convergence speed for systems compared with the finite-time control strategy. Subsequently, some extensive studies on fixed-time control issues have been conducted [20, 21]. It is noted that the abovementioned literature only studied single-layer CDNs and multiplex networks. In addition, not only is the structure of MCNs complicated, but its dynamic property is influenced significantly by all the nodes', whether they are from the same cluster in the same or a different layer or not. It is hard to apply the methods for studying the fixed-time cluster synchronization control issues of single-layer CDNs to the practical fixed-time cluster synchronization of MCNs directly. Thus, it is necessary to seek for efficient tools for dealing with the cluster synchronization control problems of MCNs.

Due to the openness of information sharing networks, MCNs are vulnerable to malicious attacks, such as denial-of-service (DoS) attacks [22], covert attacks [23], and deception attacks [24]. Such attacks may destroy the desired performance of MCNs, it is a challenging to analyze the network security problem and design appropriate controllers to against the deteriorating effect when attacks occur. Up to now, fruitful achievements about cyber attacks have been available [25, 26]. Among the

various attacks, DoS attacks destroy the integrity of communication data by evaluating the data transmitted between the sensors and the actuators, inducing packet losses in the communication channel. Many scholars are devoted to the study of DoS attacks [27, 28]. A distributed consensus for heterogeneous switched nonlinear multiagent systems under DoS attacks has been discussed in [29]. The authors of [30] studied the resilient cooperative output regulation issues of nonlinear multiagent systems with DoS attacks. In fact, exchanging information among nodes in MCNs is essential, which may be a great temptation for cyber attackers. Recent years have witnessed growing attention to the integrated design of event-triggered control, fixed-time synchronization, and anti-DoS attack strategies. For example, the authors of [31] proposed a intermittent event-triggered practical fixed-time synchronization scheme for multilayer networks, but ignored the impact of DoS attacks on communication channels. The authors in [32] addressed the fixed-time anti-DoS synchronization problem, yet the control mechanism leads to conservative communication resource utilization. The authors of [33] studied practical fixed-time synchronization using intermittent event triggering but failed to consider the nonlinear coupling characteristics of multilayer networks. These works either lack the integration of all three core elements or cannot adapt to the complex topological structure of MCNs, motivating the research in this paper. Therefore, it is meaningful and challenge to investigate the nature of MCNs under DoS attacks.

Motivated by the discussion above, this paper will investigate the practical fixed-time cluster synchronization control issue for a class of multilayer complex networks. By introducing a distributed dynamic event-triggered mechanism, cluster synchronization conditions ensuring the multilayer complex networks desired performance in fixed-time are established and controllers are proposed. As a whole, the main contributions of this paper are as follows.

(1) *A fairly general MCN model* is formulated by considering nonlinear node dynamics, different node numbers across layers, and heterogeneous nonlinear coupling effects (both intra layer and inter layer) between nodes, which can more accurately describe the structural and dynamical features of real-world MCNs compared with existing simplified models.

(2) *A resilient distributed dynamic event-triggered mechanism* is proposed. A dynamic event-triggered mechanism with an auxiliary dynamic variable is designed for MCNs under DoS attacks, which can adaptively adjust the trigger threshold, avoid over triggering caused by fixed thresholds under intermittent DoS-induced communication losses, and balance communication efficiency and synchronization control performance.

(3) *Practical fixed-time cluster synchronization control criteria* are established to accommodate the simultaneous effects of intermittent data arrivals and DoS attacks induced by a dynamic event-triggered transmission mechanism. Based on the Lyapunov stability theory and inequality techniques, sufficient algebraic conditions for the practical fixed-time cluster synchronization of MCNs under DoS attacks and the proposed dynamic event-triggered mechanism are derived. The settling time of the synchronization error converging to a bounded region is independent of the initial states of the network, and the bounded convergence region of the synchronization error is explicitly given.

The rest of this paper is organized as follows: Section 2 shows the model's description, Section 3 gives the main results. In Section 4, a numerical example is presented, and concluding remarks are given in Section 5.

2. Model description and preliminaries

2.1. Notation

Denote $\mathbb{N}$ and $\mathbb{N}^+$ as the set of natural numbers and non-negative integers, respectively. $\mathbb{R}^n$ and $\mathbb{R}^{n\times m}$ stand for the set of n-dimensional real spaces and $n \times m$ dimensional real spaces, respectively. Denote $\mathbb{I}_n \in \mathbb{R}^{n\times n}$ as an identity matrix, $n \in \mathbb{N}^+$. $\mathbb{B} > 0$ ($\mathbb{B} < 0$) means that the matrix $\mathbb{B}$ is positive definite (negative definite). The superscript T indicates matrix transposition and $\otimes$ is the Kronecker product. For a vector $x \in \mathbb{R}^n$ and a positive scalar $p \in \mathbb{N}^+$, $\|x\|$ is the Euclidean norm, $[x]^p = (|x_1|^p, \cdots, |x_n|^p)^T$, and $sign(x) = diag\{sign(x_1), \cdots, sign(x_n)\}$, where $sign(\cdot)$ is the signum function. The matrices are all with appropriate dimensions without any special description.

The interconnection topology among nodes in the same layer is modeled by a digraph $\mathbb{G}(\mathbb{V}^m, \mathbb{E}^m, A^m)$ of order $N_m \in \mathbb{N}^+$ with a set of nodes $\mathbb{V}^m = \{1, 2, \cdots, N_m\}$, a set of edges $\mathbb{E}^m \subset \mathbb{V}^m \times \mathbb{V}^m$, and weighted adjacency matrix $A^{mm} = (a_{ij}^{mm})_{N_m\times N_m} \in \mathbb{R}^{N_m\times N_m}$, where a_{ij}^{mm} is the weight of the directed edge (j, i) satisfying $a_{ij}^{mm} \neq 0$ if $(j, i) \in \mathbb{E}$ and $a_{ij}^{mm} = 0$ otherwise. Moreover, it is assumed that $a_{ii}^{mm} = 0$, $i \in \mathbb{V}^m$ to avoid self-loops.

Let $\mathbb{D} = \{1, 2, \cdots, d\}$ be a cluster set with $d \geq 1$ and $\{\mathbb{V}_1^m, \cdots, \mathbb{V}_d^m\}$ be a partition of the initial node set $\mathbb{V}^m$ such that $\mathbb{V}^m = \cup_{l=1}^d \mathbb{V}_l^m$, and $\mathbb{V}_l^m \cap \mathbb{V}_k^m = \emptyset$ for $l \neq k$, $l, k \in \mathbb{D}$. Denote $\alpha_k^m = \text{card}(\mathbb{V}_k^m)$ as the total number of the nodes in the kth cluster of the mth layer, $k \in \mathbb{D}$, $m \in \mathbb{M} = \{1, \cdots, M\}$, where $\lceil\cdot\rfloor$ represents the cardinality of the set. Denote this as

$$\begin{aligned}
&\mathbb{V}_1^m = \{\alpha_0^m + 1, \cdots, \alpha_0^m + \alpha_1^m\},\\
&\quad \cdots,\\
&\mathbb{V}_k^m = \{\alpha_0^m + \cdots + \alpha_{k-1}^m + 1, \cdots, \alpha_0^m + \cdots + \alpha_k^m\},\\
&\quad \cdots,\\
&\mathbb{V}_d^m = \{\alpha_0^m + \cdots + \alpha_{d-1}^m + 1, \cdots, \alpha_0^m + \cdots + \alpha_d^m\},\\
&\alpha_0^m = 0, \quad \sum_{k=1}^{d} \alpha_k^m = N_m.
\end{aligned}$$

Denote $\bar{N} = N_1 + \cdots + N_M$ as the total number of the nodes in the MCNs.

2.2. Modeling of MCNs

Consider a class of MCNs consisting of M layers with N_m interacting nodes in the mth layer, in which the dynamics of the ith node of the mth layer, $\forall\ i \in \mathbb{V}^m$ and $\forall\ m \in \mathbb{M}$, are described by the following coupling state-space equation:

$$\dot{x}_i^m(t) = f_k(x_i^m(t)) + \sum_{j=1}^{N_m} a_{ij}^{mm} g_{k_j}(x_j^m(t)) + r_i^m(t) + \sum_{l=1, l\neq m}^{M} c^{ml} \sum_{j=1}^{N_l} a_{ij}^{ml} g_{k_j}(x_j^l(t)) + u_i^m(t), \tag{2.1}$$

where $x_i^m(t) = (x_{i1}^m(t), \cdots, x_{i\bar{n}}^m(t))^T \in \mathbb{R}^{\bar{n}}$ is the state vector of the ith node in the mth layer; $f_k(x_i^m(t)) = (f_k(x_{i1}^m(t)), \cdots, f_k(x_{i\bar{n}}^m(t)))^T \in \mathbb{R}^{\bar{n}}$, $i \in \mathbb{V}_k^m$, $g_{k_j}(x_j^m(t)) = (g_{k_j}(x_{j1}^m(t)), \cdots, g_{k_j}(x_{j\bar{n}}^m(t)))^T \in \mathbb{R}^{\bar{n}}$: are continuous nonlinear functions; k_j denotes the cluster index of node j, i.e., $k_j = \bar{k}$ if $j \in \mathbb{V}_{\bar{k}}^m$ for layer m; or $j \in \mathbb{V}_{\bar{k}}^l$

for layer l, $\bar{k} \in \mathbb{D}$, $m, l \in \mathbb{M}$; $A^{mm} = (a_{ij}^{mm})_{N_m \times N_m} \in R^{N_m \times N_m}$ is the intra layer coupling weight matrix with $\sum_{j \in \mathbb{V}_k^m} a_{ij}^{mm} = 0$, $k \in \mathbb{D}$ and

$$A^{ml} = (a_{ij}^{ml})_{N_m \times N_l} \in R^{N_m \times N_l}$$

is the inter layer coupling weight matrix with

$$\sum_{j \in \mathbb{V}_k^l} a_{ij}^{ml} = 0, \quad k \in \mathbb{D};$$

$r_i^m(t)$ stands for the disturbance with $\|r_i^m(t)\| \leq r_i^m$, r_i^m is a known positive scalar; c^{ml} is the coupling strength between the mth layer and the lth layer with $c^{ml} = c^{lm}$; and $u_i^m(t)=(u_{i1}^m(t), \cdots, u_{i\bar{n}}^m(t))^T \in \mathbb{R}^{\bar{n}}$ is the control input of the ith node of layer m. This topological modeling framework conforms to the fundamental definition of multilayer network structure proposed by Radicchi et al. [34], which lays a unified theoretical foundation for characterizing the intra layer and inter layer connection characteristics of real-world MCNs.

Remark 2.1. *The multilayer network model described in (2.1) features significant practical relevance and generality. On one hand, the model consists of M layers, with the total number of nodes $\bar{N}$ flexibly distributed across layers according to practical application scenarios, without being restricted to the idealized assumption of a uniform number of nodes per layer. On the other hand, the coupling relationships between nodes fully consider the heterogeneous characteristics of multilayer networks. Not only do nodes in different clusters and the same cluster within the same layer have nonlinear couplings, but nodes between different layers also achieve dynamic interactions through the inter layer coupling strength c^{ml}. This design breaks through the limitation of homogeneous coupling in traditional single-layer networks and can accurately characterize the structural features of real systems such as brain networks, smart grids, and social networks, laying a practical model foundation for a subsequent analysis of cluster synchronization issues in complex scenarios.*

Our objective is to synchronize the MCNs (2.1) of $\bar{N}$ nodes with d desired heterogeneous states, which can be d different reference trajectories, d equilibrium points, d periodic orbits or d chaotic attractors, or an event in the presence of DoS attacks. For this purpose, we denote such d desired heterogeneous states as $s_k(t) \in R^{\bar{n}}$, $k \in \mathbb{D}$, which involve

$$\dot{s}_k(t) = f_k(s_k(t)). \tag{2.2}$$

Combining the MCNs in (2.1) and the heterogeneous states in (2.2), the objective is to design a suitable cluster synchronization controller $u_i^m(t)$ for each node i in each layer m belonging to the cluster $\mathbb{V}_k^m$ such that $x_i^m(t) \to s_k(t)$ for any $i \in \mathbb{V}_k^m$ and $k \in \mathbb{D}$. Thus it is clear that

$$\mathbb{S}(t) = (\overbrace{s_1(t), \cdots, s_1(t)}^{\alpha_1^1+\cdots+\alpha_1^M}, \cdots, \overbrace{s_d(t), \cdots, s_d(t)}^{\alpha_d^1+\cdots+\alpha_d^M})$$

denotes the desired cluster synchronization pattern under the proposed synchronization controller.

Assume the error $e_i^m(t) = x_i^m(t) - s_k(t)$, $i \in \mathbb{V}_k^m$, $k \in \mathbb{D}$ and $m \in \mathbb{M}$. The error network can be described as

$$\dot{e}_i^m(t) = \bar{f}_k(e_i^m(t)) + \sum_{j=1}^{N_m} a_{ij}^{mm} g_{k_j}(x_j^m(t)) + r_i^m(t) + \sum_{l=1, l\neq m}^{M} c^{ml} \sum_{j=1}^{N_l} a_{ij}^{ml} g_{k_j}(x_j^l(t)) + u_i^m(t), \tag{2.3}$$

where

$$\bar{f}_k(e_i^m(t)) = f_k(x_i^m(t)) - f_k(s_k(t)).$$

Definition 2.1. *For any initial state, if a scalar $\epsilon > 0$ exists such that*

$$\lim_{t\to T_f} \sum_{m\in\mathbb{M}} \sum_{k\in\mathbb{D}} \sum_{i\in\mathbb{V}_k^m} \|e_i^m(t)\| \le \epsilon, \tag{2.4}$$

$$\sum_{m\in\mathbb{M}} \sum_{k\in\mathbb{D}} \sum_{i\in\mathbb{V}_k^m} \|e_i^m(t)\| \le \epsilon, t \ge T_f. \tag{2.5}$$

Then the MCN (2.1) is said to be practical fixed-time cluster synchronization with the settling time T_f, which is independent of the initial value of the networks.

Furthermore, the nonlinear functions satisfy the following mild assumption.

Assumption 2.1. *The real constant matrices $F_k \in \mathbb{R}^{\bar{n}\times\bar{n}}$, $G_k \in \mathbb{R}^{\bar{n}\times\bar{n}}$, and $k \in \mathbb{D}$ exist such that for any $w, v \in \mathbb{R}^{\bar{n}}$, the following inequality holds:*

$$(w - v)^T(f_k(w) - f_k(v)) \le (w - v)^T F_k(w - v), \tag{2.6}$$

and

$$(g_k(w) - g_k(v))^T(g_k(w) - g_k(v)) \le (w - v)^T G_k(w - v). \tag{2.7}$$

Moreover, to guarantee the stability of the closed-loop system, the matrices F_k, $k \in \mathbb{D}$, are assumed to be negative definite, i.e., $\lambda_{\max}(F_k) < 0$, where $\lambda_{\max}(\cdot)$ denotes the maximum eigenvalue.

2.3. Dynamic event-triggered mechanism and DoS attacks

In the following, a dynamic event-triggered mechanism is considered, under which the cluster synchronization controller can be updated in an intermittent manner. For any $i \in \mathbb{V}^m$, $m \in \mathbb{M}$, let the triggering sequence be denoted as $\{t_{i,q}^m\}_{q=1}^{+\infty}$ with $0 = t_{i,1}^m < t_{i,2}^m < \cdots < t_{i,q}^m < \cdots$. The following triggering mechanism specifies how the triggering times can be recursively determined

$$t_{i,q+1}^m = \begin{cases} \inf\{t > t_{i,q}^m | \zeta^T(e_i^m(t), e_i^m(t_{i,q}^m))\zeta(e_i^m(t), e_i^m(t_{i,q}^m)) \\ \quad - \nu_{i1}^m(e_i^m(t))^T e_i^m(t) - \nu_{i2}^m \eta_i^m(t) \ge 0\}, \ \ \text{ACK} = 1, \\ t_{i,q}^m + \bar{\delta}, \ \ \text{ACK} = 0, \end{cases} \tag{2.8}$$

where ν_{i1}^m, $\nu_{i2}^m > 0$, $i \in \mathbb{V}^m$, $m \in \mathbb{M}$, and ACK is the acknowledgment of transmission signal. ACK can be used to detect whether there is data dropout or not due to the occurrence of unknown attacks, $\bar{\delta} > 0$ is the sampling period when there is data dropout, and

$$\begin{aligned} \zeta(e_i^m(t), e_i^m(t_{i,q}^m)) =& \xi_{i1}^m e_i^m(t_{i,q}^m) - \xi_{i1}^m e_i^m(t) + \xi_{i2}^m (e_i^m(t_{i,q}^m))^{\bar{p}} - \xi_{i2}^m sign(e_i^m(t))[e_i^m(t)]^{\bar{p}} \\ &+ \xi_{i3}^m (e_i^m(t_{i,q}^m))^{\bar{q}} - \xi_{i3}^m sign(e_i^m(t))[e_i^m(t)]^{\bar{q}}, \end{aligned} \tag{2.9}$$

where $\xi_{ij}^m > 0$, $j = 1, 2, 3$, $i \in \mathbb{V}^m$, $m \in \mathbb{M}$, $\bar{p} \in (0, 1)$, $\bar{q} > 1$, $\epsilon \in (0, 1)$, and $\eta_i^m(t)$ is an auxiliary dynamic variable satisfying

$$\begin{aligned} \dot{\eta}_i^m(t) =& -\theta_{i1}^m \eta_i^m(t) - \theta_{i2}^m (\eta_i^m(t))^{\frac{\bar{p}+1}{2}} - \theta_{i3}^m (\eta_i^m(t))^{\frac{\bar{q}+1}{2}} - \theta_{i4}^m (\zeta(e_i^m(t), e_i^m(t_{i,q}^m)))^T \zeta(e_i^m(t), e_i^m(t_{i,q}^m)) \\ &- \nu_{i1}^m (e_i^m(t))^T e_i^m(t)), \end{aligned} \tag{2.10}$$

where $\eta_i^m(0) = \eta_{i,0}^m > 0$, $\theta_{ij}^m > 0$, $j = 1, 2, 3, 4$, $i \in \mathbb{V}^m$, $m \in \mathbb{M}$.

Compared with static event-triggering, the dynamic mechanism introduces the auxiliary variable $\eta_i^m(t)$ to adaptively adjust the trigger threshold—this advantage is critical under sporadic DoS-induced communication losses, as it avoids over trigging caused by fixed thresholds when data transmission is intermittently interrupted and mitigates the conservatism of static mechanisms in balancing communication efficiency and synchronization performance.

Remark 2.2. *The event-triggering function $\zeta(\cdot, \cdot)$ in (2.9) is designed with three distinct terms: A linear term, a term with the exponent $\bar{p} < 1$, and a term with exponent $\bar{q} > 1$. This structure is not a mere complication but is intentionally aligned with the fixed-time control law in (2.12). According to fixed-time stability theory [19, 20], the term with $\bar{p} < 1$ is responsible for ensuring fast convergence when the error is small, while the term with $\bar{q} > 1$ guarantees that the convergence time remains bounded even for large initial errors. The linear term provides the baseline exponential stability and facilitates the Lyapunov analysis. By embedding these three components into the triggering function, the event-triggered sampling error can be effectively compensated in the Lyapunov derivative (see Eq (3.10)), thereby enabling the derivation of the fixed-time synchronization conditions in Theorem 3.1.*

Remark 2.3. *The negative sign in front of the $\theta_{i4}^m \zeta^T \zeta$ term in (2.10) is intentionally designed. Unlike conventional dynamic event-triggered mechanisms where the auxiliary variable serves as a positive threshold, here $\eta_i^m(t)$ acts as a decaying factor that accelerates triggering when the triggering error ζ is large. This design ensures that communication becomes more frequent when needed, and it also simplifies the Lyapunov analysis by allowing the $\zeta^T \zeta$ terms from the controller and the η-dynamics to combine into a negative definite contribution (see the proof of Theorem 3.1). Moreover, the non-negativity of $\eta_i^m(t)$ is not required for stability; the Lyapunov function $V(t)$ remains valid even if $\eta_i^m(t)$ becomes temporarily negative.*

Remark 2.4. *The triggered condition (2.8) means that the data packet of the ith node in layer m satisfying $\zeta^T(e_i^m(t), e_i^m(t_{i,q}^m))\zeta(e_i^m(t), e_i^m(t_{i,q}^m)) - \nu_{i1}^m(e_i^m(t))^T e_i^m(t) - \nu_{i2}^m \eta_i^m(t) < 0$ during $[t_{i,q}^m, t_{i,q+1}^m)$ when* ACK $= 1$ *will not be sent to the controller, which will reduce the load of network transmission compared with the time-triggered mechanism and the static event-triggered mechanism. Combined with (2.10), it yields*

$$\dot{\eta}_i^m(t) > -(\theta_{i1}^m + \theta_{i4}^m \nu_{i2}^m)\eta_i^m(t) - \theta_{i2}^m(\eta_i^m(t))^{\frac{\bar{p}+1}{2}} - \theta_{i3}^m(\eta_i^m(t))^{\frac{\bar{q}+1}{2}}$$

with $\eta_i^m(0) = \eta_{i,0}^m > 0$. Suppose, for contradiction, that a first time instant $t^* > 0$ exists such that $\eta_i^m(t^*) = 0$ and $\eta_i^m(t) > 0$ for all $t \in [0, t^*)$. By the definition of the right-hand derivative, this implies

$$\dot{\eta}_i^m(t_+^*) = \lim_{h \to 0^+} \frac{\eta_i^m(t^* + h) - \eta_i^m(t^*)}{h} \leq 0,$$

since $\eta_i^m(t^* + h)$ must be negative for a sufficiently small $h > 0$ by the definition of t^* as the first zero crossing. However, substituting $\eta_i^m(t^*) = 0$ into the aforementioned strict lower bound gives

$$\dot{\eta}_i^m(t^*) > -(\theta_{i1}^m + \theta_{i4}^m \nu_{i2}^m) \cdot 0 - \theta_{i2}^m \cdot 0 - \theta_{i3}^m \cdot 0 = 0,$$

which directly contradicts $\dot{\eta}_i^m(t_+^*) \leq 0$. Therefore, no such t^* exists, and we conclude $\eta_i^m(t) > 0$ for all $t \geq 0$.

In a network environment, MCNs can be affected by DoS attacks that destroy the information interaction between communication channels. Let the starting instants' sequence of DoS attacks be $\{h_n\}$, $n \in \mathbb{N}$, with $h_0 > 0$; that is, the time instants at which the signal transmission fails. For DoS attacks, define the nth active and inactive intervals as

$$\mathbb{H}_n = \{h_n\} \cup [h_n, h_n + \kappa_n),$$
$$\mathbb{I}_n = [h_n + \kappa_n, h_{n+1}),$$

where κ_n is the length of the nth DoS attack.

For the DoS attacks, the following assumptions are given.

Assumption 2.2. *[28] The scalars $n_0 > 0$ and $\kappa_f \in (0, 1)$ exist. For any $t_2 > t_1 \geq 0$, let $N_f(t_2, t_1)$ denote the number of DoS attacks in $[t_1, t_2)$ such that $N_f(t_2, t_1) \leq n_0 + \kappa_f(t_2 - t_1)$.*

Assumption 2.3. *[28] A scalar $n_1 > 0$ exists. Denote κ_a as the average duration of each attack for the network. For any $t_2 > t_1 \geq 0$, let $|H(t_2, t_1)|$ denote the the length of the DoS duration in $[t_1, t_2)$ such that $|H(t_2, t_1)| \leq n_1 + \kappa_a(t_2 - t_1)$.*

The ideal DoS interval suggests the interval when the network is interrupted due to DoS attack, and the ideal scenario implies that the networks can transmit information when the DoS attack disappears. Since the instants at which the DoS attacks are inactive are unknown, the current state information cannot be promptly transmitted at the end moments $h_n + \kappa_n$ of the DoS attack. Thus, for the ith node in layer m, define the equivalent DoS attack interval and the DoS attack-free interval as $\bar{\mathbb{H}}_{i,n}^m$ and $\bar{\mathbb{I}}_{i,n}^m$, corresponding to $\mathbb{H}_n$ and $\mathbb{I}_n$, and let $\bar{h}_{i,n}^m \in [h_n + \kappa_n, h_n + \kappa_n + \bar{\delta})$ represent the ending moment of DoS.

Remark 2.5. *According to the definition of the average control rate and the elasticity number in [20], denote $\bar{\kappa} \in (0, 1)$ as the average non attack rate and $|\bar{\mathbb{I}}_i^m(t_2, t_1)|$ as the actual non attack length of the ith node in layer m during the interval $[t_1, t_2)$. On the basis of Assumptions 2.2 and 2.3, Eq (2.12), and by following the resilient control framework for DoS attacks [35, 36], we have*

$$\begin{aligned} |\bar{\mathbb{I}}_i^m(t_2, t_1)| &= t_2 - t_1 - |\bar{\mathbb{H}}_i^m(t_2, t_1)| \\ &\geq t_2 - t_1 - |H_i^m(t_2, t_1)| - N_f(t_2, t_1)\bar{\delta} \\ &\geq t_2 - t_1 - n_1 - \kappa_a(t_2 - t_1) - N_f(t_2, t_1)\bar{\delta} \\ &\geq t_2 - t_1 - n_1 - \kappa_a(t_2 - t_1) - (n_0 + \kappa_f(t_2 - t_1))\bar{\delta} \\ &= \bar{\kappa}(t_2 - t_1) - T_\kappa, \end{aligned} \tag{2.11}$$

where $\bar{\kappa} = 1 - \kappa_a - \kappa_f\bar{\delta}$, $T_\kappa = n_1 + n_0\bar{\delta}$.

Taking both the dynamic event-triggered mechanism and DoS attacks in consideration, assume that there are $\bar{l}_{i,q}^m \in \mathbb{N}$ triggers for the ith node in the layer m over the time span $(\bar{h}_{i,n}^m, h_{n+1})$, and takes $t_{i,q}^m = \bar{h}_{i,n}^m$, $t_{i,q+\bar{l}_{i,q}^m+1} = h_{n+1}$. The widely adopted synchronization controller then takes the following form:

$$u_i^m(t) = \begin{cases} 0, \ \ t \in \bar{\mathbb{H}}_{i,n}^m, \\ -\xi_{i1}^m e_i^m(t_{i,q+l}^m) - \xi_{i2}^m \text{sign}(e_i^m(t_{i,q+l}^m))[e_i^m(t_{i,q+l}^m)]^{\bar{p}} - \xi_{i3}^m \text{sign}(e_i^m(t_{i,q+l}^m))[e_i^m(t_{i,q+l}^m)]^{\bar{p}}, \\ t \in \bar{\mathbb{I}}_{i,n}^m \cap [t_{i,q+l}^m, t_{i,q+l+1}^m), \ l = 0, \cdots, \bar{l}_{i,q}^m, \end{cases} \tag{2.12}$$

where the parameters are defined as before.

Remark 2.6. *In (2.12), the control input is set to zero during DoS attack intervals $\bar{\mathbb{H}}_{i,n}^{m}$. This is a common and theoretically convenient choice, as it leads to a clean exponential bound on the Lyapunov function during attacks. Alternative strategies, such as holding the last successful control value or using model-based predictions, could potentially improve performance but introduce significant analytical challenges. The hold strategy, for instance, would require bounding the mismatch between the held control and the current optimal control, which is particularly delicate in fixed-time control due to the nonlinear power terms. The zero-input strategy represents a worst-case design that ensures stability under the most adverse conditions. If additional information about the attack pattern is available, less conservative strategies could be explored; this is an interesting direction for future research.*

Before ending this section, some important lemmas are given.

Lemma 2.1. *[37] If $w, v \in \mathbb{R}^n$, then*

$$w^T v + v^T w \leq \iota w^T w + \iota^{-1} v^T v, \quad \iota > 0. \tag{2.13}$$

Lemma 2.2. *[37] For $x_i \geq 0,\ i = 1, \cdots, n,\ \bar{p} \in (0, 1],\ \bar{q} > 1$, then*

$$\sum_{i=1}^{n} x_i^{\bar{p}} \geq (\sum_{i=1}^{n} x_i)^{\bar{p}}, \quad \sum_{i=1}^{n} x_i^{\bar{q}} \geq n^{1-\bar{q}} (\sum_{i=1}^{n} x_i)^{\bar{q}}.$$

Lemma 2.3. *[20] Assume that the continuous function $V(t) \geq 0$ satisfies*

$$\dot{V}(t) \leq \begin{cases} -\varsigma_1 V^{\phi}(t) - \varsigma_2 V^{\varphi}(t) \varsigma_3 V(t) + \varepsilon, t \in [t_{2p}, t_{2p+1}), \\ \varsigma_4 V(t) + \varepsilon, t \in [t_{2p+1}, t_{2p+2}), \end{cases} \tag{2.14}$$

where $\varsigma_i > 0,\ i = 1, \cdots, 4,\ \phi > 1,\ \varphi \in (0, 1),\ \varepsilon > 0$. If there are positive constants $\bar{\varsigma}$ and $\hat{\varsigma} \in (0, 1)$ satisfying the following inequalities:

$$\varsigma_3 - \bar{\varsigma}(1 - \hat{\varsigma}) > 0,\ \bar{\varsigma}\hat{\varsigma} - \varsigma_4 > 0,$$

then, $V(t)$ converges to the attraction region in a fixed-time T_f, and

$$\left\{ \lim_{t \to T_f} e(t) | V(t) \leq \max\{\mu_1, \mu_2, \mu_3\} \right\},$$

where $\mu_1 = \rho/\bar{\varsigma}_4$, $\rho = \varepsilon \exp\{\bar{\varsigma} T_p\}$, $\bar{\varsigma}_4 = \bar{\varsigma}\hat{\varsigma} - \varsigma_4$, $\mu_2 = (\rho/((1 - \varrho)\bar{\varsigma}_1))^{1/\phi}$, $\bar{\varsigma}_1 = \varsigma_1 \exp\{(1 - \phi)\bar{\varsigma} T_\varsigma\}$, $\mu_3 = (\rho/((1 - \varrho)\varsigma_2))^{1/\varphi}$, $\varrho \in (0, 1)$, and

$$T_f \leq \frac{1 + \bar{\varsigma}_1 \varrho(\phi - 1) T_\varsigma}{\bar{\varsigma}_1 \varrho(\phi - 1)\hat{\varsigma}} + \frac{1 + \varsigma_2 \varrho(1 - \varphi) T_\varsigma}{\varsigma_2 \varrho(1 - \varphi) T_\varsigma},$$

in which T_ς is the elasticity number and $\hat{\varsigma}$ is the average control rate.

Remark 2.7. *Lemma 2.1 enables the decomposition of coupling terms into quadratic forms; Lemma 2.2 facilitates the combination of low-power and high-power terms in the Lyapunov analysis; and Lemma 2.3 provides the fundamental framework for analyzing systems with alternating stable and unstable modes caused by DoS attacks. These lemmas are essential tools that transform the complex nonlinear dynamics into tractable algebraic conditions.*

3. Main results

The main purpose of this section is to investigate under what type of conditions, the nodes in the same cluster synchronize to the desired trajectories in fixed time.

For convenience, some notation is given as follows:

$$\begin{aligned}
\bar{g}_{k_j}(e_j^m(t)) &= g_{k_j}(x_j^m(t)) - g_{k_j}(s_k(t)), j \in \mathbb{V}_k^m,\\
E(t) &= ((e_1^1(t))^T, \cdots, (e_{N_1}^1(t))^T, \cdots, (e_1^M(t))^T, \cdots, (e_{N_M}^M(t))^T)^T,\\
\bar{F} &= \mathrm{diag}\{\mathrm{F}_{\mathrm{N}_1}, \mathrm{F}_{\mathrm{N}_2}, \cdots, \mathrm{F}_{\mathrm{N}_\mathrm{M}}\},\\
F_{N_m} &= \mathrm{diag}\{\mathrm{F}_1 \otimes \mathrm{I}_{\alpha_1^\mathrm{m}}, \cdots, \mathrm{F}_\mathrm{d} \otimes \mathrm{I}_{\alpha_\mathrm{d}^\mathrm{m}}\},\ \mathrm{m} \in \mathbb{M},\\
\bar{G} &= \mathrm{diag}\{\mathrm{G}_{\mathrm{N}_1}, \mathrm{G}_{\mathrm{N}_2}, \cdots, \mathrm{G}_{\mathrm{N}_\mathrm{M}}\},\\
G_{N_m} &= \mathrm{diag}\{\mathrm{G}_1 \otimes \mathrm{I}_{\alpha_1^\mathrm{m}}, \cdots, \mathrm{G}_\mathrm{d} \otimes \mathrm{I}_{\alpha_\mathrm{d}^\mathrm{m}}\},\ \mathrm{m} \in \mathbb{M},\\
\bar{A} &= (\bar{A}^{ml})_{M\times M}, \quad \bar{A}^{ml} = (\bar{a}_{ij}^{ml})_{N_m\times N_l},\ m, l \in \mathbb{M},\\
\bar{a}_{ij}^{ml} &= \begin{cases} a_{ij}^{ml}, & l = m,\\ c^{ml}a_{ij}^{ml}, & l \neq m. \end{cases}
\end{aligned}$$

Now, a theorem about practical fixed-time cluster synchronization issue of MCNs (2.1) is presented.

Theorem 3.1. *Under Assumptions 2.1–2.3, given the positive constants n_1, n_0, $\bar{\delta}$, κ_a, κ_f, $\eta_{i,0}^m$, if the positive scalars ν_{i1}^m, ν_{i2}^m, ξ_{ij}^m, $j = 1, 2, 3$, θ_{ij}^m, $j = 1, \cdots, 4$, $\bar{\varsigma}$, $i \in \mathbb{V}^m$, $m \in \mathbb{M}$, ι_1, and ι_2, such that*

$$\min\{\epsilon_1, \epsilon_2, \epsilon_3\} > 0, \tag{3.1}$$

$$\epsilon_1 - \bar{\varsigma}(1 - \bar{\kappa}) > 0, \tag{3.2}$$

$$\bar{\varsigma}\bar{\kappa} - \epsilon_5 > 0, \tag{3.3}$$

where

$$\begin{aligned}
\epsilon_1 &= \min\{\bar{\epsilon}_1 - \lambda_1 - \theta_4, \theta_1 - \nu_2\}, \quad \epsilon_2 = \min\{2^{\frac{\bar{p}+1}{2}}\xi_2, \theta_2\},\\
\epsilon_3 &= 2^{\frac{1-\bar{q}}{2}}\min\{\xi_3(\bar{n}\bar{N})^{\frac{1-\bar{q}}{2}}2^{\frac{\bar{q}+1}{2}}, \theta_3\bar{N}^{\frac{1-\bar{q}}{2}}\}, \quad \epsilon_5 = \lambda_1 + 2\theta_4,\\
\lambda_1 &= \lambda_{\max}\{2\bar{F} + \iota_1 I_{\bar{n}\bar{N}} + \iota_2(\bar{A} \otimes I_{\bar{n}})(\bar{A} \otimes I_{\bar{n}})^T + \iota_2^{-1}\bar{G}\},\\
\bar{\epsilon}_1 &= \min\{2\xi_{i1}^m - \nu_{i1}^m - 1, i \in \mathbb{V}^m, m \in \mathbb{M}\},\\
\theta_4 &= \max\{\theta_{i4}^m\nu_{i1}^m, i \in \mathbb{V}^m, m \in \mathbb{M}\},\\
\theta_j &= \min\{\theta_{ij}^m, i \in \mathbb{V}^m, m \in \mathbb{M}\}, \quad j = 1, 2, 3,\\
\nu_2 &= \max\{\frac{1}{2}\nu_{i2}^m, i \in \mathbb{V}^m, m \in \mathbb{M}\}, \quad \xi_2 = \min\{\xi_{i2}^m, i \in \mathbb{V}^m, m \in \mathbb{M}\},\\
\xi_3 &= \min\{\xi_{i3}^m, i \in \mathbb{V}^m, m \in \mathbb{M}\}, \quad \bar{\kappa} = 1 - \kappa_a - \kappa_f\bar{\delta},
\end{aligned}$$

then MCNs (2.1) under the dynamic event-triggered mechanism (2.8) with (2.9), (2.10), and the controller (2.12) can achieve practical fixed-time cluster synchronization; moreover, the cluster synchronization error $e_i^m(t)$, $i \in \mathbb{V}^m$, $m \in \mathbb{M}$, converges to the region as follows in a fixed-time T_f;

$$\left\{\lim_{t\to T_f}\|e_i^m(t)\| | V(t) \leq \max\{\bar{\mu}_1, \bar{\mu}_2, \bar{\mu}_3\}\right\},$$

where $\bar{\mu}_1 = \bar{\rho}/\bar{\epsilon}_5$, $\bar{\mu}_2 = (\bar{\rho}/((1-\varrho)\bar{\epsilon}_3))^{2/(\bar{q}+1)}$, $\bar{\mu}_3 = (\bar{\rho}/((1-\varrho)\epsilon_2))^{2/(1+\bar{p})}$, $\bar{\rho} = \epsilon_4 \exp\{\bar{\varsigma} T_\kappa\}$, $\bar{\epsilon}_5 = \bar{\varsigma}\bar{\kappa} - \epsilon_5$, $\varrho \in (0,1)$, $\bar{\epsilon}_3 = \epsilon_3 \exp\{(1-\bar{q})\bar{\varsigma} T_\kappa/2\}$, $\epsilon_4 = r^2\bar{N}/(2\iota_1)$, $r = \max\{r_i^m, i \in \mathbb{V}^m, m \in \mathbb{M}\}$, $T_\kappa = n_1 + n_0\bar{\delta}$, *and* T_f *satisfies the following inequality,*

$$T_f \leq \frac{2 + \epsilon_2\varrho(1-\bar{p})T_\kappa}{\epsilon_2\varrho(1-\bar{p})\bar{\kappa}} + \frac{2 + \bar{\epsilon}_3\varrho(\bar{q}-1)T_\kappa}{\bar{\epsilon}_3\varrho(\bar{q}-1)\bar{\kappa}}.$$

Proof. Select the Lyapunov function $V(t) = V_1(t) + V_2(t)$, and

$$V_1(t) = \frac{1}{2}\sum_{m=1}^{M}\sum_{i=1}^{N_m}(e_i^m(t))^T e_i^m(t), \tag{3.4}$$

$$V_2(t) = \sum_{m=1}^{M}\sum_{i=1}^{N_m}\eta_i^m(t). \tag{3.5}$$

From Lemma 2.2, for $t \in \bar{\mathbb{I}}_{i,n}^m \cap [t_{i,q+o}^m, t_{i,q+o+1}^m)$, $o = 0, \cdots, \bar{l}_{i,q}^m$, we have

$$\begin{aligned}\dot{V}_1(t) = &\sum_{m=1}^{M}\sum_{i=1}^{N_m}(e_i^m(t))^T \bar{f}_k(e_i^m(t) + \sum_{m=1}^{M}\sum_{i=1}^{N_m}(e_i^m(t))^T r_i^m(t) + \sum_{m=1}^{M}\sum_{i=1}^{N_m}\sum_{j=1}^{N_m}(e_i^m(t))^T a_{ij}^{mm} g_{k_j}(x_j^m(t))\\ &+ \sum_{m=1}^{M}\sum_{i=1}^{N_m}\sum_{l=1,l\neq m}^{M}\sum_{j=1}^{N_l} c^{ml}(e_i^m(t))^T a_{ij}^{ml} g_{k_j}(x_j^l(t)) + \sum_{m=1}^{M}\sum_{i=1}^{N_m}(e_i^m(t))^T u_i^m(t)\end{aligned} \tag{3.6}$$

and

$$\begin{aligned}\dot{V}_2(t) = \sum_{m=1}^{M}\sum_{i=1}^{N_m}\dot{\eta}_i^m(t) = &\sum_{m=1}^{M}\sum_{i=1}^{N_m}(-\theta_{i1}^m\eta_i^m(t) - \theta_{i2}^m|\eta_i^m(t)|^{\frac{\bar{p}+1}{2}} - \theta_{i3}^m|\eta_i^m(t)|^{\frac{\bar{q}+1}{2}})\\ &- \sum_{m=1}^{M}\sum_{i=1}^{N_m}\theta_{i4}^m\zeta^T(e_i^m(t), e_i^m(t_{i,q+o}^m))\zeta(e_i^m(t), e_i^m(t_{i,q+o}^m)).\end{aligned} \tag{3.7}$$

From (2.6) and (2.10), one gets

$$\begin{aligned}\dot{V}_1(t) &\leq \sum_{m=1}^{M}\sum_{i=1}^{N_m}(e_i^m(t))^T F_k e_i^m(t) + \frac{\iota_1}{2}\sum_{m=1}^{M}\sum_{i=1}^{N_m}(e_i^m(t))^T e_i^m(t)\\ &\quad + \frac{r^2\bar{N}}{2\iota_1} + \sum_{m=1}^{M}\sum_{i=1}^{N_m}\sum_{l=1}^{M}\sum_{j=1}^{N_l}(e_i^m(t))^T \bar{a}_{ij}^{ml}\bar{g}_{k_j}(e_j^l(t)) + \sum_{m=1}^{M}\sum_{i=1}^{N_m}(e_i^m(t))^T u_i^m(t)\\ &\leq \frac{1}{2}E^T(t)(2\bar{F} + \iota_1 I_{\bar{n}\bar{N}} + \iota_2(\bar{A}\otimes I_{\bar{n}})(\bar{A}\otimes I_{\bar{n}})^T + \iota_2^{-1}\bar{G})E(t) + \frac{r^2\bar{N}}{2\iota_1} + \sum_{m=1}^{M}\sum_{i=1}^{N_m}(e_i^m(t))^T u_i^m(t)\\ &\leq \lambda_1 V_1(t) + \epsilon_4 + \sum_{m=1}^{M}\sum_{i=1}^{N_m}(e_i^m(t))^T u_i^m(t)\end{aligned} \tag{3.8}$$

and

$$\dot{V}_2(t) \leq -\theta_1 V_2(t) - \theta_2 V_2^{\frac{\bar{p}+1}{2}}(t) - \theta_3\bar{N}^{\frac{1-\bar{q}}{2}(t)}V_2^{\frac{\bar{q}+1}{2}}(t) + \sum_{m=1}^{M}\sum_{i=1}^{N_m}\theta_{i4}\nu_{i1}^m\|e_i^m(t)\|^2. \tag{3.9}$$

Given the dynamic event-triggered mechanism (2.8) with (2.9), (2.10), the controller (2.12), and Lemma 2.2, this yields

$$\begin{aligned}(e_i^m(t))^T u_i^m(t) &= (e_i^m(t))^T(-\xi_{i1}^m e_i^m(t_{i,q+o}^m) - \xi_{i2}^m(e_i^m(t_{i,q+o}^m))^{\bar{p}} - \xi_{i3}^m(e_i^m(t_{i,q+o}^m))^{\bar{q}})\\ &= (e_i^m(t))^T(-\zeta(e_i^m(t), e_i^m(t_{i,q}^m)) - \xi_{i1}^m e_i^m(t) - \xi_{i2}^m sign(e_i^m(t))(e_i^m(t))^{\bar{p}}\\ &\quad - \xi_{i3}^m sign(e_i^m(t))(e_i^m(t))^{\bar{q}}))\\ &\le \frac{1}{2}(\zeta(e_i^m(t), e_i^m(t_{i,q+o}^m)))^T\zeta(e_i^m(t), e_i^m(t_{i,q+o}^m)) + \frac{1}{2}(e_i^m(t))^T e_i^m(t) - \xi_{i1}^m\|e_i^m(t)\|^2\\ &\quad - \xi_{i2}^m\sum_{r=1}^{\bar{n}}((e_{ir}^m(t))^2)^{\frac{\bar{p}+1}{2}} - \xi_{i3}^m\sum_{r=1}^{\bar{n}}((e_{ir}^m(t))^2)^{\frac{\bar{q}+1}{2}}\\ &\le -(\xi_{i1}^m - \frac{1}{2}\nu_{i1}^m - \frac{1}{2})\|e_i^m(t)\|^2 + \frac{1}{2}\nu_{i2}^m\eta_i^m(t) - \xi_{i2}^m\|e_i^m(t)\|^{\bar{p}+1} - \xi_{i3}^m\bar{n}^{\frac{1-\bar{q}}{2}}\|e_i^m(t)\|^{\bar{q}+1}.\end{aligned} \tag{3.10}$$

Combining (3.8) with (3.10), we can deduce that

$$\begin{aligned}\dot{V}(t) \le{}& \lambda_1 V_1(t) + \epsilon_4 - \sum_{m=1}^{M}\sum_{i=1}^{N_m}(\xi_{i1}^m - \frac{1}{2}\nu_{i1}^m - \frac{1}{2})\|e_i^m(t)\|^2 - \sum_{m=1}^{M}\sum_{i=1}^{N_m}\xi_{i2}^m\|e_i^m(t)\|^{\bar{p}+1}\\ &- \sum_{m=1}^{M}\sum_{i=1}^{N_m}\xi_{i3}^m\bar{n}^{\frac{1-\bar{q}}{2}}\|e_i^m(t)\|^{\bar{q}+1} + \frac{1}{2}\sum_{m=1}^{M}\sum_{i=1}^{N_m}\nu_{i2}^m\eta_i^m(t) + \sum_{m=1}^{M}\sum_{i=1}^{N_m}\theta_{i4}\nu_{i1}^m\|e_i^m(t)\|^2\\ &- \theta_1 V_2(t) - \theta_2 V_2^{\frac{\bar{p}+1}{2}}(t) - \theta_3\bar{N}^{\frac{1-\bar{q}}{2}(t)}V_2^{\frac{\bar{q}+1}{2}}(t),\end{aligned} \tag{3.11}$$

and then

$$\begin{aligned}\dot{V}(t) &\le -(\bar{\epsilon}_1 - \lambda_1 - \theta_4)V_1(t) - 2^{\frac{\bar{p}+1}{2}}\xi_2 V_1^{\frac{\bar{p}+1}{2}}(t) - 2^{\frac{\bar{q}+1}{2}}\xi_3(\bar{n}\bar{N})^{\frac{1-\bar{q}}{2}}V_1^{\frac{\bar{p}+1}{2}}(t) - (\theta_1 - \nu_2)V_2(t)\\ &\quad - \theta_2 V_2^{\frac{\bar{p}+1}{2}}(t) - \theta_3(\bar{N})^{\frac{1-\bar{q}}{2}}V_2^{\frac{\bar{q}+1}{2}}(t) + \epsilon_4\\ &\le -\epsilon_1 V(t) - \epsilon_2 V^{\frac{\bar{p}+1}{2}}(t) - \epsilon_3 V^{\frac{\bar{q}+1}{2}}(t) + \epsilon_4.\end{aligned} \tag{3.12}$$

On the other hand, for $t \in \bar{\mathbb{H}}_{i,n}^m$, one can get

$$\begin{aligned}\dot{V}(t) &= \lambda_1 V_1(t) + \epsilon_4 + \sum_{m=1}^{M}\sum_{i=1}^{N_m}\dot{\eta}_i^m(t)\\ &\le \lambda_1 V_1(t) + \epsilon_4 + \sum_{m=1}^{M}\sum_{i=1}^{N_m}\theta_{i4}\nu_{i1}^m\|e_i^m(t)\|^2\\ &\le \epsilon_5 V(t) + \epsilon_4.\end{aligned} \tag{3.13}$$

Hence, from (3.12) and (3.13), we obtain

$$\dot{V}(t) \le \begin{cases} -\epsilon_1 V(t) - \epsilon_2 V^{\frac{\bar{p}+1}{2}}(t) - \epsilon_3 V^{\frac{\bar{q}+1}{2}}(t) + \epsilon_4, t \in \bar{\mathbb{T}}_{i,n}^m \cap [t_{i,q+l}^m, t_{i,q+l+1}^m),\ l = 0, \cdots, \bar{l}_{i,q}^m,\\ \epsilon_5 V(t) + \epsilon_4, t \in \bar{\mathbb{H}}_{i,n}^m,\end{cases} \tag{3.14}$$

which implies that MCNs (2.1) can achieve the practical fixed-time cluster synchronization in a fixed-time T_f according to Lemma 2.3. □

Remark 3.1. *Theorem 3.1 provides practical fixed-time cluster synchronization criteria which are in form of an algebraic inequality for MCNs under DoS attacks and a dynamic event-triggered mechanism.*

Remark 3.2. *Under typical operating conditions where the disturbance bound r and the attack parameters $n_0, n_1, \kappa_a, \kappa_f$ are known, the synchronization error $\|e_i^m(t)\|$ after the settling time T_f is approximately bounded by*

$$\|e_i^m(t)\| \lesssim \max\left\{\frac{\epsilon_4}{\bar{\zeta}\bar{\kappa}-\epsilon_5}, \left(\frac{\epsilon_4}{\epsilon_2}\right)^{\frac{2}{1+\bar{p}}}, \left(\frac{\epsilon_4}{\epsilon_3}\right)^{\frac{2}{1+\bar{q}}}\right\},$$

where the exponential terms $\exp\{\bar{\zeta}T_k\}$ *have been absorbed into the constants by considering worst-case scenarios.*

Remark 3.3. *The feasibility conditions in Theorem 3.1 define the boundary of guaranteed practical fixed-time synchronization. When the parameters are chosen close to this boundary (e.g., $\epsilon_1 \approx \bar{\zeta}(1-\bar{\kappa})$ or $\epsilon_2 \approx 0$), the synchronization performance degrades significantly: The ultimate error bound increases sharply and the settling time grows without bound. Therefore, in practical implementations, it is advisable to maintain adequate safety margins.*

In event-triggered control systems, the Zeno phenomenon refers to the situation where an infinite number of triggering events occur in a finite time interval [38, 39]. This behavior is undesirable because it would require the controller to update infinitely quickly, making its practical implementation impossible. Therefore, excluding Zeno behavior is a fundamental requirement for any event-triggered control scheme to be physically realizable. In the following, Theorem 3.2 proves that under the conditions of Theorem 3.1, the proposed dynamic event-triggered mechanism guarantees a positive lower bound on inter event intervals, thereby excluding Zeno behavior.

Theorem 3.2. *Under the conditions (3.1) and (3.3) in Theorem 3.1, there is no Zeno behavior in MCNs (2.1) under the dynamic event-triggered mechanism (2.8) with (2.9), and (2.10).*

Proof. According to Theorem 3.1, a positive scalar $\Lambda_1 > 0$ exists such that for $\forall t > 0$, $\|e_i^m(t)\| \le \Lambda_1$. Thus, we have

$$\begin{aligned}\|\dot{\zeta}(e_i^m(t), e_i^m(t_{i,q}^m))\| &= \|\left(-\xi_{i1}^m I_n - \xi_{i2}^m \bar{p}\, sign(e_i^m(t))[e_i^m(t)]^{\bar{p}-1} \ -\xi_{i3}^m \bar{q}\, sign(e_i^m(t))[e_i^m(t)]^{\bar{q}-1}\right)\dot{e}_i^m(t)\| \\ &\le \Lambda_2\|\bar{f}_k(e_i^m(t)) + \sum_{l=1}^{M}\sum_{j=1}^{N_l}\bar{a}_{ij}^{ml} g_{k_j}(e_j^l(t)) + r_i^m(t) + u_i^m(t)\| \qquad (3.15)\\ &\le \Lambda_3 + \Lambda_2 z_i^m(t_{i,q}^m),\end{aligned}$$

where

$$\begin{aligned}\Lambda_2 &= \xi_{i1}^m + \xi_{i2}^m\bar{p}\Lambda_1^{\bar{p}-1} + \xi_{i3}^m\bar{q}\Lambda_1^{\bar{q}-1},\\ \Lambda_3 &= \Lambda_1\Lambda_2(\max\{\|F_k\|, k\in\mathbb{D}\} + \|\bar{A}\| + r),\\ z_i^m(t_{i,q}^m) &= \|\xi_{i1}^m e_i^m(t_{i,q+l}^m) + \xi_{i2}^m(e_i^m(t_{i,q+l}^m))^{\bar{p}} + \xi_{i3}^m(e_i^m(t_{i,q+l}^m))^{\bar{q}}\|.\end{aligned}$$

From the dynamic event-triggered mechanism (2.8), when $t = t^m_{i,q+1}$, this yields

$$\zeta^T(e^m_i(t^m_{i,q+1}), e^m_i(t^m_{i,q}))\zeta(e^m_i(t^m_{i,q+1}), e^m_i(t^m_{i,q})) - \nu^m_{i1}(e^m_i(t^m_{i,q+1}))^T e^m_i(t^m_{i,q+1}) - \nu^m_{i2}\eta^m_i(t^m_{i,q+1}) = 0. \tag{3.16}$$

Due to (3.15) and (3.16), we can get the following inequality:

$$(\bar{z}^m_i(t^m_{i,q+1}))^{1/2} \leq (\Lambda_3 + \Lambda_2 z^m_i(t^m_{i,q}))(t^m_{i,q+1} - t^m_{i,q}), \tag{3.17}$$

where

$$\bar{z}^m_i(t^m_{i,q+1}) = \nu^m_{i1}(e^m_i(t^m_{i,q+1}))^T e^m_i(t^m_{i,q+1}) + \nu^m_{i2}\eta^m_i(t^m_{i,q+1}) > 0.$$

From (3.18), we have

$$\Delta t^m_{i,q} = t^m_{i,q+1} - t^m_{i,q} \geq \frac{(\bar{z}^m_i(t^m_{i,q+1}))^{1/2}}{\Lambda_3 + \Lambda_2 z^m_i(t^m_{i,q})} > 0, \tag{3.18}$$

which implies that Zeno behavior will not occur in the MCNs (2.1) under the dynamic event-triggered mechanism (2.8) with (2.9), and (2.10). □

According to Theorem 3.1, we can easily derive the practical fixed-time cluster synchronization condition for MCNs without DoS attacks. The related dynamic event-triggered mechanism without DoS attacks can be presented as follows:

$$t^m_{i,q+1} = \inf\{t > t^m_{i,q} | \zeta^T(e^m_i(t), e^m_i(t^m_{i,q}))\zeta(e^m_i(t), e^m_i(t^m_{i,q}))\nu^m_{i1}(e^m_i(t))^T e^m_i(t) - \nu^m_{i2}\eta^m_i(t) \geq 0\}. \tag{3.19}$$

Corollary 3.1. *Under Assumption 2.1, given the positive constant $\eta^m_{i,0}$, if the positive scalars ν^m_{i1}, ν^m_{i2}, ξ^m_{ij}, $j = 1, 2, 3$, θ^m_{ij}, $j = 1, \cdots, 4$, $i \in \mathbb{V}^m$, $m \in \mathbb{M}$, ι_1, ι_2 exist such that*

$$\min\{\epsilon_1, \epsilon_2, \epsilon_3\} > 0, \tag{3.20}$$

where the parameters are defined as Theorem 3.1, then MCNs (2.1) under the dynamic event-triggered mechanism (3.19) with (2.9), and (2.10), and the controller (2.12) can achieve practical fixed-time cluster synchronization; moreover, the cluster synchronization error $e^m_i(t)$, $i \in \mathbb{V}^m$, $m \in \mathbb{M}$, converges to the region as follows in a fixed-time T_f:

$$\left\{\lim_{t \to T_f} \|e^m_i(t)\| | V(t) \leq \max\{\tilde{\mu}_1, \tilde{\mu}_2, \tilde{\mu}_3\}\right\},$$

where $\tilde{\mu}_1 = \epsilon_4/(\epsilon_1(1-\varrho))$, $\tilde{\mu}_2 = (\epsilon_4/((1-\varrho)\epsilon_3))^{2/(1+\bar{q})}$, $\tilde{\mu}_3 = (\epsilon_4/((1-\varrho)\epsilon_2))^{2/(1+\bar{p})}$, $\varrho \in (0,1)$, and T_f satisfies the following inequality,

$$T_f \leq \max\{T_1, T_2, T_3\},$$

where

$$T_1 = \frac{2ln(1+\varrho\epsilon_1/\epsilon_2)}{\epsilon_1\varrho(1-\bar{p})} + \frac{2ln(1+\varrho\epsilon_1/\epsilon_3)}{\epsilon_1\varrho(\bar{q}-1)},$$
$$T_2 = \frac{2ln(1+\epsilon_1/(\varrho\epsilon_2))}{\epsilon_1(1-\bar{p})} + \frac{2ln(1+\epsilon_1/\epsilon_3)}{\epsilon_1(\bar{q}-1)},$$
$$T_3 = \frac{2ln(1+\epsilon_1/\epsilon_2)}{\epsilon_1(1-\bar{p})} + \frac{2ln(1+\epsilon_1/(\varrho\epsilon_3))}{\epsilon_1(\bar{q}-1)}.$$

It is worth mentioning that the dynamic event-triggered mechanism in (2.8) includes the static one as a special case. In addition, the results for practical fixed-time cluster synchronization of the MCNs (2.1) under a static event-triggered mechanism can be developed straightforwardly from Theorem 3.1 by letting ν_{i2}^m approach to 0. Such a static event-triggered mechanism can be described by

$$t_{i,q+1}^m = \begin{cases} \inf\{t > t_{i,q}^m | \zeta^T(e_i^m(t), e_i^m(t_{i,q}^m))\zeta(e_i^m(t), e_i^m(t_{i,q}^m)) - \nu_{i1}^m(e_i^m(t))^T e_i^m(t) \geq 0\}, & \text{ACK} = 1, \\ t_{i,q}^m + \bar{\delta}, & \text{ACK} = 0. \end{cases} \tag{3.21}$$

The design criterion for practical fixed-time cluster synchronization of the MCNs (2.1) under the abovementioned static event-triggered mechanism is stated as follows. The proof is omitted for reasons of space.

Corrollary 3.2. *Under Assumptions 2.1–2.3, given the positive constants n_1, n_0, $\bar{\delta}$, κ_a, κ_f, if the positive scalars ν_{i1}^m, ξ_{ij}^m, $j = 1, 2, 3$, $\bar{\varsigma}$, $i \in \mathbb{V}^m$, $m \in \mathbb{M}$, ι_1, and ι_2 exist such that*

$$\min\{\hat{\epsilon}_1, \hat{\epsilon}_2, \hat{\epsilon}_3\} > 0, \tag{3.22}$$

$$\hat{\epsilon}_1 - \bar{\varsigma}(1 - \bar{\kappa}) > 0, \tag{3.23}$$

$$\bar{\varsigma}\bar{\kappa} - \hat{\epsilon}_5 > 0, \tag{3.24}$$

where the parameters are defined as Theorem 3.1, and

$$\begin{aligned} \hat{\epsilon}_1 &= \min\{2\xi_{i1}^m - \nu_{i1}^m - \lambda_1 - 1, i \in \mathbb{V}^m, m \in \mathbb{M}\}, \\ \hat{\epsilon}_2 &= 2^{\frac{1+\bar{p}}{2}} \min\{\xi_{i2}^m, i \in \mathbb{V}^m, m \in \mathbb{M}\}, \\ \hat{\epsilon}_3 &= 2^{\frac{1+\bar{q}}{2}} (\bar{n}\bar{N})^{\frac{1-\bar{q}}{2}} \min\{\xi_{i3}^m, i \in \mathbb{V}^m, m \in \mathbb{M}\}, \end{aligned}$$

and $\hat{\epsilon}_5 = \lambda_1$, then MCNs (2.1) under the static event-triggered mechanism (3.21) and the controller (2.12) can achieve practical fixed-time cluster synchronization. Moreover, the cluster synchronization error $e_i^m(t)$, $i \in \mathbb{V}^m$, $m \in \mathbb{M}$, converges to the region as follows in a fixed-time T_f:

$$\left\{ \lim_{t \to T_f} \|e_i^m(t)\| | V(t) \leq \max\{\hat{\mu}_1, \hat{\mu}_2, \hat{\mu}_3\} \right\},$$

where

$$\begin{aligned} &\hat{\mu}_1 = \bar{\rho}/(\bar{\varsigma}\bar{\kappa} - \hat{\epsilon}_5), \quad \hat{\mu}_2 = (\bar{\rho}/((1 - \varrho)\hat{\epsilon}_3 \exp\{(1 - \bar{q})\bar{\varsigma}T_\kappa/2\}))^{2/(1+\bar{q})}, \\ &\hat{\mu}_3 = (\bar{\rho}/((1 - \varrho)\hat{\epsilon}_2))^{2/(1+\bar{p})}, \quad \breve{\epsilon}_3 = \hat{\epsilon}_3 \exp\{(1 - \bar{q})\bar{\varsigma}T_\kappa/2\}, \end{aligned}$$

and T_f satisfies the following inequality:

$$T_f \leq \frac{2 + \hat{\epsilon}_2\varrho(1 - \bar{p})T_\kappa}{\hat{\epsilon}_2\varrho(1 - \bar{p})\bar{\kappa}} + \frac{2 + \breve{\epsilon}_3\varrho(\bar{q} - 1)T_\kappa}{\breve{\epsilon}_3\varrho(\bar{q} - 1)\bar{\kappa}}.$$

In what follows, we present a result enabling the co-design of the dynamic event-triggered parameters and the controller's gain in a unified viewpoint.

Theorem 3.3. *Under Assumptions 2.1–2.3, given the positive constants n_1, n_0, $\bar{\delta}$, κ_a, κ_f, and $\eta_{i,0}^m$, if the positive scalars $\hat{\xi}_1$, $\hat{\nu}_1$, $\hat{\theta}_4$, $\hat{\nu}_2$, $\hat{\theta}_1$, $\bar{\varsigma}$, ι_1, and ι_2 exist such that*

$$(2\hat{\xi} - \hat{\nu}_1 - \hat{\theta}_4 - \iota_1)I_{\bar{n}\bar{N}} - \Gamma > 0, \tag{3.25}$$

$$2\hat{\xi} - \hat{\nu}_1 - \hat{\theta}_4 - \bar{\varsigma}\kappa_a\kappa_f > 0, \tag{3.26}$$

$$\hat{\theta}_1 - \hat{\nu}_2 - \bar{\varsigma}\kappa_a\kappa_f > 0, \tag{3.27}$$

$$(\bar{\varsigma}(1 - \kappa_a\kappa_f) - 2\hat{\theta}_4 - \iota_1)I_{\bar{n}\bar{N}} - \Gamma > 0, \tag{3.28}$$

where

$$\Gamma = 2\bar{F} + \iota_2(\bar{A} \otimes I_{\bar{n}})(\bar{A} \otimes I_{\bar{n}})^T + \iota_2^{-1}\bar{G},$$

then MCNs (2.1) can achieve practical fixed-time cluster synchronization with $\max\{\xi_{i1}^m, i \in \mathbb{V}^m, m \in \mathbb{M}\} \leq \hat{\xi}_1$, $\min\{\xi_{i2}^m, \xi_{i3}^m, i \in \mathbb{V}^m, m \in \mathbb{M}\} > 0$, $\max\{\theta_{i1}^m, i \in \mathbb{V}^m, m \in \mathbb{M}\} \leq \hat{\theta}_1$, $\min\{\theta_{i2}^m, \theta_{i3}^m, i \in \mathbb{V}^m, m \in \mathbb{M}\} > 0$, $\max\{\theta_{i4}^m, i \in \mathbb{V}^m, m \in \mathbb{M}\} \leq \theta_4\hat{\nu}_1^{-1}$, $\max\{\nu_{i1}^m, i \in \mathbb{V}^m, m \in \mathbb{M}\} \leq \hat{\nu}_1$, $\max\{\nu_{i2}^m, i \in \mathbb{V}^m,$ *and* $m \in \mathbb{M}\} \leq 2\hat{\nu}_2$.

The theorem can be conducted from Theorem 3.1, thus we omit the proof here.

4. An illustrative example

In this section, we present a numerical example to validate the effectiveness of the proposed theoretical results. The MCN model considered here captures the essential features of real-world interconnected systems, such as smart grids and transportation networks, where multiple layers (e.g., communication layers or physical layers) interact through nonlinear couplings. The DoS attack pattern is designed as a periodic on-off signal, which is a widely adopted model in the literature for its simplicity in demonstrating theoretical validity. The attack parameters are chosen according to typical assumptions in resilient control studies. Incorporating real-world attack traces or more sophisticated stochastic models remains an important direction for future research. Consider a MCN with three layers of nine nodes that are assigned into two clusters. Figure 1 shows the topological structure of the MCN.

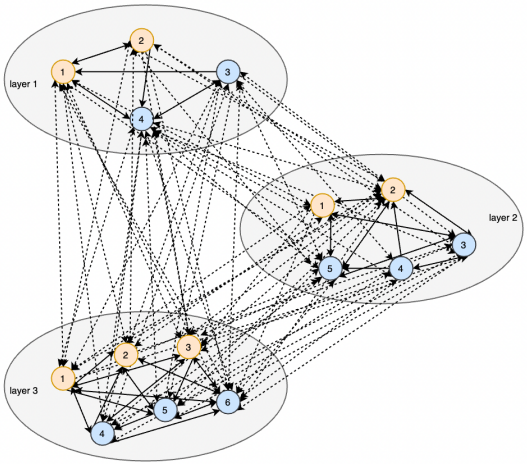

Figure 1. The topological structure of the MCN.

The network parameters of the MCN are given as follows:

$$A^{11}=\begin{bmatrix}-1&1&1&-1\\2&-2&0&0\\0&0&-1&1\\1&-1&2&-2\end{bmatrix},\quad A^{12}=\begin{bmatrix}1&-1&0&0&0\\-1&1&0.2&0&-0.2\\0&0&0.3&0.5&-0.8\\0.2&-0.2&-1.2&1&0.2\end{bmatrix},\quad A^{13}=\begin{bmatrix}1&-0.5&-0.5&0.2&0&-0.2\\0.5&-0.5&0&0&0&0\\0&0&0&-1&0.5&0.5\\0.5&-0.2&-0.3&1&0.2&-1.2\end{bmatrix},$$

$$A^{21}=\begin{bmatrix}1&-1&0&0\\1&-1&-0.2&0.2\\0&0&-1&1\\0&0&1&-1\\0.2&-0.2&1&-1\end{bmatrix},\quad A^{22}=\begin{bmatrix}-1&1&1&0&-1\\2&-2&-1&0.5&0.5\\1&-1&-2&1&1\\0&0&1&-1&0\\-1&1&0.5&0.5&-1\end{bmatrix},\quad A^{23}=\begin{bmatrix}1&-1&0&0&0&0\\0.5&-1&0.5&0.2&0&-0.2\\1&-0.5&-0.5&0&0&0\\0&0&0&1&-0.5&-0.5\\0.2&0&-0.2&0.5&-1&0.5\end{bmatrix},$$

$$A^{33}=\begin{bmatrix}-1&0&1&1&0&-1\\1&-1&0&0.5&0.5&-1\\2&0&-2&-1&0&1\\1&0&-1&-2&2&0\\0.5&-1&0.5&0&-1&1\\0.5&0.5&-1&0.5&0.5&-1\end{bmatrix},\quad A^{31}=\begin{bmatrix}1&-1&-0.5&0.5\\0.5&-0.5&0&0\\1&-1&0&0\\0&0&1&-1\\0&0&0.8&-0.8\\0.2&-0.2&1.2&-1.2\end{bmatrix},\quad A^{32}=\begin{bmatrix}1&-1&0&0&0\\0.5&-0.5&0&0&0\\-2&2&0.2&-0.1&-0.1\\0&0&1&-0.5&-0.5\\0&0&-1&0.5&0.5\\0.2&-0.2&1&0&-1\end{bmatrix};$$

and

$$\begin{aligned}
f_1(x_i^m)&=(-0.6x_{i1}^m-\tanh(1.8x_{i1}^m)+0.08x_{i2}^m,\ -0.8x_{i2}^m-\tanh(2.2x_{i2}^m)+0.08x_{i1}^m)^T;\\
f_2(x_i^m)&=(-0.4x_{i1}^m-\ tanh(2.5(x_{i1}^m-3))+0.05x_{i2}^m,\ -1.0x_{i2}^m-\tanh(2.8(x_{i2}^m+3))+0.05x_{i1}^m)^T;\\
g_1(x_i^m)&=(0.2x_{i1}^m,\quad 0.2x_{i2}^m)^T,i\in\mathbb{V}_1^m,m=1,2,3;\\
g_2(x_i^m)&=(0.1x_{i1}^m,\quad 0.1x_{i2}^m)^T,i\in\mathbb{V}_2^m,m=1,2,3;\\
r_i^1(\cdot)&=(0.01\sin(x_{i1}^m),0.02\cos(x_{i2}^m))^T,i\in\mathbb{V}^1;\\
r_i^2(\cdot)&=(0.02\tanh(x_{i1}^m),0.05\sin(x_{i2}^m))^T,i\in\mathbb{V}^2;\\
r_i^3(\cdot)&=(0.03\sin(x_{i1}^m),0.05\cos(x_{i2}^m))^T,i\in\mathbb{V}^3;\\
c^{12}&=c^{21}=0.1,\quad c^{13}=c^{31}=0.05,\quad c^{23}=c^{32}=0.08,
\end{aligned}$$

where $x_i^m=(x_{i1}^m,x_{i2}^m)^T\in\mathbb{R}^2$, $m=1,2,3$, and $\eta_i^m(0)=1$, $i\in\mathbb{V}^m$, $m=1,2,3$. The initial values of the MCNs and the cluster leader $s_k(t)$, $k=1,2$, are set as follows:

$$\begin{aligned}
&x_1^1(0)=\begin{bmatrix}3\\-1\end{bmatrix},\quad x_2^1(0)=\begin{bmatrix}2\\-3\end{bmatrix},\quad x_3^1(0)=\begin{bmatrix}1\\-2\end{bmatrix},\\
&x_4^1(0)=\begin{bmatrix}-1\\1\end{bmatrix},\quad x_1^2(0)=\begin{bmatrix}1\\-2\end{bmatrix},\quad x_2^2(0)=\begin{bmatrix}2\\-1\end{bmatrix},\\
&x_3^2(0)=\begin{bmatrix}3\\-3\end{bmatrix},\quad x_4^2(0)=\begin{bmatrix}-1\\-2\end{bmatrix},\quad x_5^2(0)=\begin{bmatrix}-2\\-1\end{bmatrix},\\
&x_1^3(0)=\begin{bmatrix}-1\\-1\end{bmatrix},\quad x_2^3(0)=\begin{bmatrix}2\\-2\end{bmatrix},\quad x_3^3(0)=\begin{bmatrix}1\\-3\end{bmatrix},\\
&x_4^3(0)=\begin{bmatrix}1\\1\end{bmatrix},\quad x_5^3(0)=\begin{bmatrix}-1\\2\end{bmatrix},\quad x_6^3(0)=\begin{bmatrix}3\\3\end{bmatrix},\\
&s_1(0)=\begin{bmatrix}-2\\2\end{bmatrix},\quad s_2(0)=\begin{bmatrix}3\\-3\end{bmatrix}.
\end{aligned}$$

The attack intervals are set as $\cup_{l=0}^{+\infty}[l,l+0.1)$, then the average non attack rate = 0.9. Moreover, we can select $\bar{\delta}=0.01$, $n_0=0.1$, $\kappa_f=0.01$, $n_1=0.1$, $\kappa_a=0.01$, and then $\bar{\kappa}=0.9899$, and $T_\kappa=0.101$. To choose $\nu_{i1}^m=0.2$, $i\in\mathbb{V}^m$, $m=1,2,3$; $\nu_{i2}^m=0.3$, $\xi_{i1}^m=5$, $\xi_{i2}^m=0.8$, $\xi_{i3}^m=0.8$, $\theta_{i1}^m=8$, $\theta_{i2}^m=1$, $\theta_{i3}^m=1$, $\theta_{i4}^m=0.2$, $i\in\mathbb{V}_1^m$, $m=1,2,3$; $\nu_{i2}^m=0.5$, $\xi_{i1}^m=4.5$, $\xi_{i2}^m=0.7$, $\xi_{i3}^m=0.7$, $\theta_{i1}^m=12$, $\theta_{i2}^m=1.2$, $\theta_{i3}^m=1.2$, $\theta_{i4}^m=0.2$, $i\in\mathbb{V}_2^m$, $m=1,2,3$; $\bar{p}=0.5$, $\bar{q}=1.5$, $\bar{\varsigma}=5$, $\varrho=0.5$, and $\iota_1=\iota_2=2$. It follows that $\varepsilon_1=6.5$, $\varepsilon_2\approx 0.88$, $\varepsilon_3\approx 0.72$, $\varepsilon_5=2.5$, $\min\{\varepsilon_1,\varepsilon_2,\varepsilon_3\}>0$, $\varepsilon_1-\bar{\varsigma}(1-\bar{\kappa})=6.4495>0$, and $\bar{\varsigma}\bar{\kappa}-\varepsilon_5=2.4495>0$, which verify that the conditions of Theorem 3.1 are all satisfied.

According to Theorem 3.1, the MCN under the controller and dynamic event-triggered mechanism is a practical fixed-time cluster synchronization with

$$T_f\le 22s,\quad \bar{\mu}_1\approx 0.025,\quad \bar{\mu}_2\approx 0.28,\quad \bar{\mu}_3\approx 0.08,\quad \text{and}\quad \max\{\bar{\mu}_1,\bar{\mu}_2,\bar{\mu}_3\}=0.28.$$

The corresponding simulation results are shown in Figures 2–5. From Figures 2 and 3, we can conclud that the nodes distributed in different layers in the same cluster are cluster synchronized. The trajectories of cluster errors are

$$e_1^{xs} = \sqrt{\sum_{m=1}^{3} \sum_{i\in\mathbb{V}_1^m} (e_i^m(t))^T (e_i^m(t))},$$

and

$$e_2^{xs} = \sqrt{\sum_{m=1}^{3} \sum_{i\in\mathbb{V}_2^m} (e_i^m(t))^T (e_i^m(t))}$$

are described in Figure 4. Figure 5 shows the event-triggering instants of partial nodes in the MCN under the DoS attacks. By comparing Figure 5 with the transient error dynamic in Figures 3 and 4, we observe a clear correlation: Immediately after each DoS attack ends, the synchronization error spikes due to communication interruptions, which, in turn, triggers a burst of event triggers as the nodes attempt to compensate for the accumulated error. Figure 6 describes the trajectories of errors $e_i^m(t)$, $i \in \mathbb{V}^m$, $m = 1, 2, 3$ for the MCN without controllers.

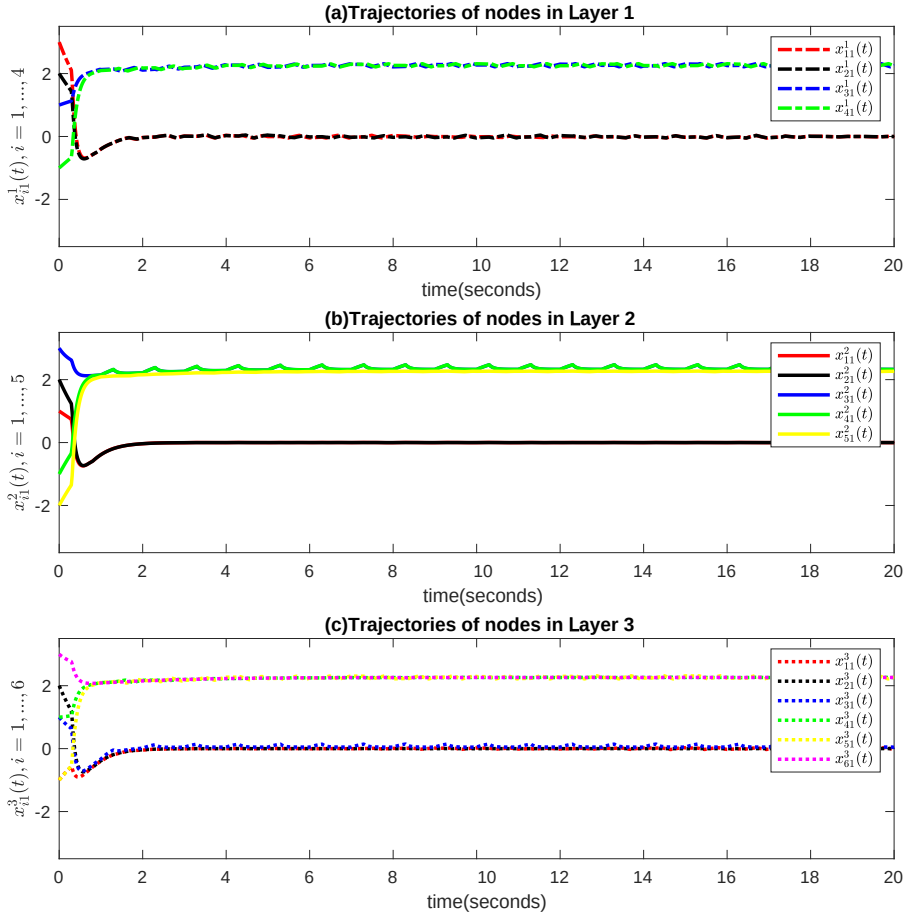

Figure 2. Transient behaviors of $x_{i1}^m(t)$, $i \in \mathbb{V}^m$, $m = 1, 2, 3$ for the MCN.

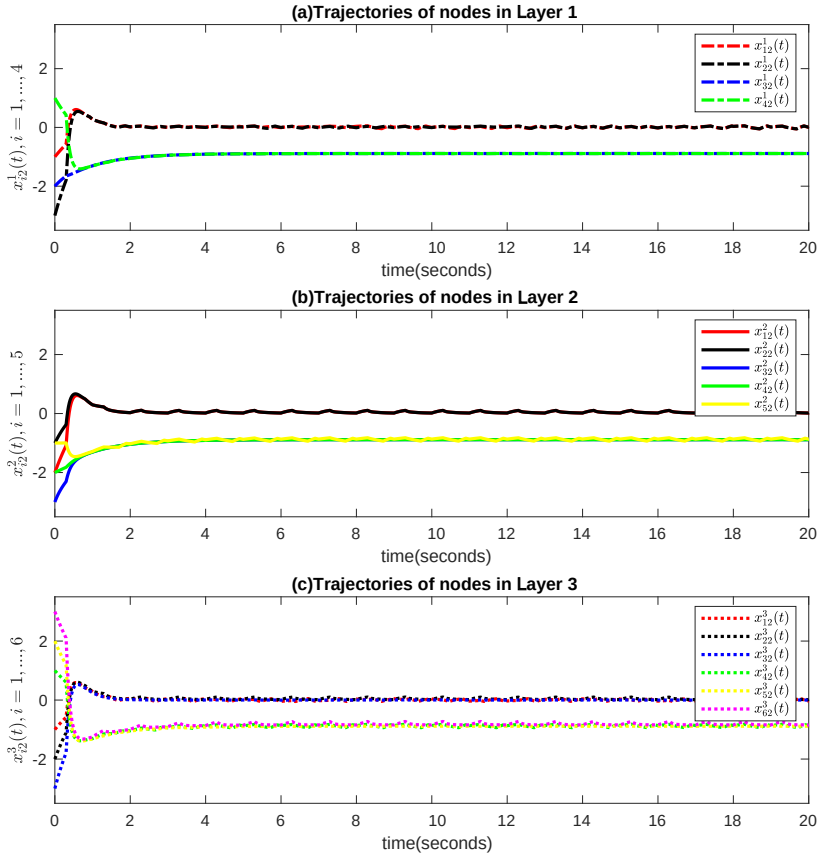

Figure 3. Transient behaviors of $x_{i2}^{m}(t)$, $i \in \mathbb{V}^{m}$, $m = 1, 2, 3$ for the MCN.

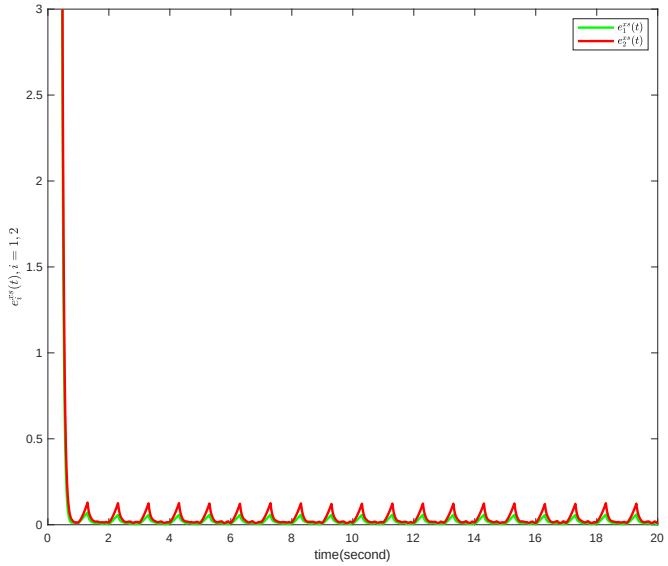

Figure 4. Trajectories of cluster errors $e_i^{xs}(t), i = 1, 2$.

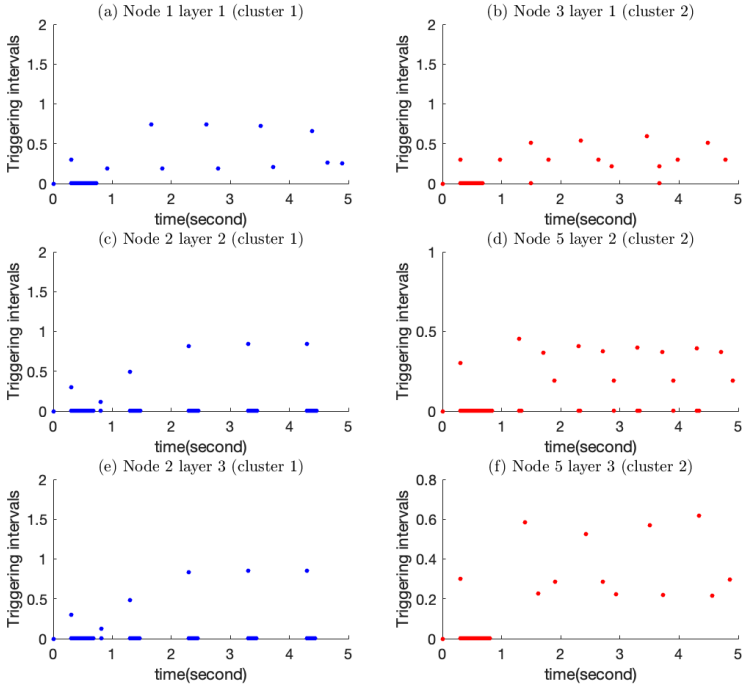

Figure 5. Dynamic event-triggered release times.

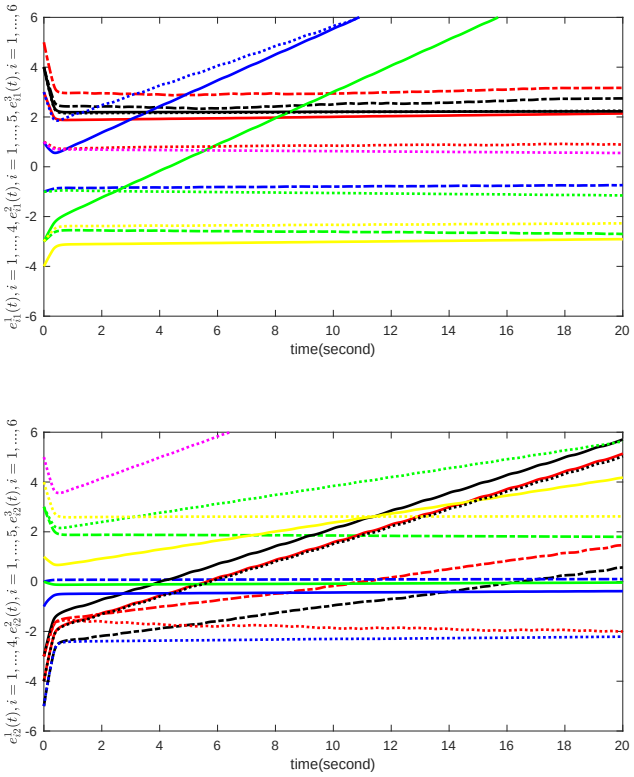

Figure 6. Trajectories of errors $e_i^m(t)$, $i \in \mathbb{V}^m$, $m = 1, 2, 3$ for the MCN without controllers.

5. Conclusions

This paper investigates the practical fixed-time cluster synchronization control problem for heterogeneous MCNs with nonlinear intra-layer and inter-layer couplings under DoS attacks. By seamlessly integrating a distributed dynamic event-triggered mechanism and anti-DoS resilience design, we address the core challenges of communication efficiency, structural complexity, and attack robustness in MCNs. Specifically, sufficient conditions for practical fixed-time cluster synchronization through Lyapunov stability theory are established, ensuring that the synchronization error converges to a bounded region within a fixed time, independent of the initial conditions. An illustrative numerical example, combined with a comparative analysis against representative existing algorithms, further validates the effectiveness and superiority of the proposed theoretical framework and control schemes. Although the proposed method effectively solves the practical fixed-time cluster synchronization problem of MCNs under DoS attacks, it has limitations, such as idealized DoS attack models, network modeling that does not consider dynamic characteristics like time delays and topological time-variation, and conservative control strategies. In the future, we will improve the dynamic network modeling, explore more general attack models, and develop integrated defense strategies that combine attack detection, isolation, and adaptive control to enhance the security and robustness of MCNs in real-world engineering scenarios.

Use of Generative-AI tools declaration

The author declares she has not used artificial intelligence (AI) tools in the creation of this article.

Acknowledgements

This work is partially supported by the Foundation for Distinguished Young Talents in Higher Education of Guangdong (2022KQNCX040) and the Youth Doctor 'Sailing' Project of Guangzhou Basic Research Plan for Basic and Applied Basic Research (grant number 1749529).

Conflict of interest

The author declares that she has no conflict of interest.

References

1. Y. Wu, H. Guo, L. Xue, N. Gunasekaran, J. Liu, Prescribed-time synchronization of stochastic complex networks with high-gain coupling, *IEEE Trans. Circuits Syst. II*, **70** (2023), 4133–4137. https://doi.org/10.1109/TCSII.2023.3271150
2. W. Tang, Y. Sheng, Q. Xiao, T. Huang, Z. Zeng, Synchronization of complex dynamical networks on time scales via intermittent dynamic event-triggered control, *IEEE Trans. Syst. Man Cybern.*, **54** (2024), 2897–2906. https://doi.org/10.1109/TSMC.2024.3352074
3. X. Wu, X. Wu, C. Wang, B. Mao, J. Lu, J. Lv, et al., Synchronization in multiplex networks, *Phys. Rep.*, **1060** (2024), 1–54. https://doi.org/10.1016/j.physrep.2024.01.005

4. M. De Domenico, More is different in real-world multilayer networks, *Nat. Phys.*, **19** (2023), 1247–1262. https://doi.org/10.1038/s41567-023-02132-1
5. X. Zhang, H. Li, Y. Yu, L. Zhang, H. Jiang, Quasi-projective and complete synchronization of discrete-time fractional-order delayed neural networks, *Neural Networks*, **164** (2023), 497–507. https://doi.org/10.1016/j.neunet.2023.05.005
6. D. Wang, W. Chen, L. Qiu, Synchronization of diverse agents via phase analysis, *Automatica*, **159** (2024), 113255. https://doi.org/10.1016/j.automatica.2023.111325
7. M. Li, X. Yang, X. Li, Delayed impulsive control for lag synchronization of delayed neural networks involving partial unmeasurable states, *IEEE Trans. Neural Networks Learn. Syst.*, **35** (2024), 783–791. https://doi.org/10.1109/TNNLS.2022.3177234
8. W. Chen, X. Wang, F. Ren, Z. Zeng, Quasi-synchronization for variable-order fractional complex dynamical networks with hybrid delay-dependent impulses, *Neural Networks*, **173** (2024), 106161. https://doi.org/10.1016/j.neunet.2024.106161
9. T. Weng, X. Chen, Z. Ren, J. Xu, H. Yang, Multiple moving agents on complex networks: from intermittent synchronization to complete synchronization, *Phys. A*, **614** (2023), 128562. https://doi.org/10.1016/j.physa.2023.128562
10. L. M. Pecora, T. L. Carroll, Master stability functions for synchronized coupled systems, *Phys. Rev. Lett.*, **80** (1998), 2109–2112. https://doi.org/10.1103/PhysRevLett.80.2109
11. M. Y. Chen, Some simple synchronization criteria for complex dynamical networks, *IEEE Trans. Circuits Syst. II*, **53** (2006), 1185–1189. https://doi.org/10.1109/TCSII.2006.882363
12. J. Yao, Z. H. Guan, D. J. Hill, Passivity-based control and synchronization of general complex dynamical networks, *Automatica*, **45** (2009), 2107–2113. https://doi.org/10.1016/j.automatica.2009.05.006
13. Y. Han, W. Lu, T. Chen, Intralayer synchronization and interlayer quasi-synchronization in multiplex networks of nonidentical layers, *IEEE Trans. Neural Networks Learn. Syst.*, **36** (2025), 3165–3174. https://doi.org/10.1109/TNNLS.2023.3326629
14. X. Yin, R. Xiao, H. Dai, Q. Zhu, Y. Sun, Influence of layer similarity on the synchronization of multiplex networks with random topologies, *IEEE Trans. Syst. Man Cybern.*, **53** (2023), 7089–7098. https://doi.org/10.1109/TSMC.2023.3290674
15. S. Zhai, W. X. Zheng, Stability conditions for cluster synchronization in directed networks of diffusively coupled nonlinear systems, *IEEE Trans. Circuits Syst.*, **70** (2023), 413–423. https://doi.org/10.1109/TCSI.2022.3208000
16. J. Li, Z. Wang, R. Lu, Y. Xu, Cluster synchronization control for discrete-time complex dynamical networks: When data transmission meets constrained bit rate, *IEEE Trans. Neural Networks Learn. Syst.*, **34** (2023), 2554–2568. https://doi.org/10.1109/TNNLS.2021.3106947
17. Y. Li, J. Zhang, J. Lu, J. Lou, Finite-time synchronization of complex networks with partial communication channels failure, *Inf. Sci.*, **634** (2023), 539–549. https://doi.org/10.1016/j.ins.2023.03.077
18. Y. Xu, Q. Gao, C. Xie, X. Zhang, X. Wu, Finite-time synchronization of complex networks with privacy-preserving, *IEEE Trans. Circuits Syst. II*, **70** (2023), 4103–4107. https://doi.org/10.1109/TCSII.2023.3274634

19. A. Polyakov, Nonlinear feedback design for fixed-time stabilization of linear control systems, *IEEE Trans. Autom. Control*, **57** (2012), 2106–2110. https://doi.org/10.1109/TAC.2011.2179869

20. J. Liu, Z. Xu, L. Xue, Y. Wu, C. Sun, Practical fixed-time synchronization of multilayer networks via intermittent event-triggered control, *IEEE Trans. Syst. Man Cybern.*, **54** (2024), 2626–2637. https://doi.org/10.1109/TSMC.2023.3341847

21. T. Wu, J. Liu, L. Xue, Y. Wu, Fixed-time synchronization of multilayer complex networks under Denial-of-Service attacks, *IEEE Trans. Circuits Syst.*, **70** (2023), 3519–3523. https://doi.org/10.1109/TCSII.2023.3261405

22. X. Ge, Q. Han, Q. Wu, X. Zhang, Resilient and safe platooning control of connected automated vehicles against intermittent Denial-of-Service attacks, *IEEE/CAA J. Autom. Sin.*, **10** (2023), 1234–1251. https://doi.org/10.1109/JAS.2022.105845

23. X. Li, P. Zhang, H. Dong, A robust covert attack strategy for a class of uncertain cyber-physical systems, *IEEE Trans. Autom. Control*, **69** (2024), 1983–1990. https://doi.org/10.1109/TAC.2023.3319071

24. Q. Liu, J. Wang, Y. Ni, C. Zhang, L. Shi, J. Qin, Performance analysis for cyber-physical systems under two types of stealthy deception attacks, *Automatica*, **160** (2024), 111446. https://doi.org/10.1016/j.automatica.2024.111446

25. L. Zhou, M. Huang, F. Tan, Y. Zhang, Mean-square bounded synchronization of complex networks under deception attacks via pinning impulsive control, *Nonlinear Dyn.*, **111** (2023), 11243–11259. https://doi.org/10.1007/s11071-023-08448-0

26. J. Li, Y. Huang, H. Rao, Y. Xu, R. Lu, Finite-time cluster synchronization for complex dynamical networks under FDI attack: A periodic control approach, *Neural Networks*, **165** (2023), 228–237. https://doi.org/10.1016/j.neunet.2023.04.013

27. C. Deng, X. Jin, Z. Wu, W. Che, Data-driven-based cooperative resilient learning method for nonlinear MASs under DoS attacks, *IEEE Trans. Neural Networks Learn. Syst.*, **35** (2024), 12107–12116. https://doi.org/10.1109/TNNLS.2023.3252080

28. Y. Wang, H. Wang, J. Xiao, Z. Guan, Synchronization of complex dynamical networks under recoverable attacks, *Automatica*, **46** (2010), 197–203. https://doi.org/10.1016/j.automatica.2009.10.024

29. S. Guo, X. Zhao, H. Wang, N. Xu, Distributed consensus of heterogeneous switched nonlinear multiagent systems with input quantization and DoS attacks, *Appl. Math. Comput.*, **456** (2023), 128127. https://doi.org/10.1016/j.amc.2023.128127

30. D. Zhang, C. Deng, G. Feng, Resilient cooperative output regulation for nonlinear multiagent systems under DoS attacks, *IEEE Trans. Autom. Control*, **68** (2023), 2521–2528. https://doi.org/10.1109/TAC.2022.3184388

31. J. Liu, Z. H. Xu, L. Xue, Y. B. Wu, C. Y. Sun, Practical fixed-time synchronization of multilayer networks via intermittent event-triggered control, *IEEE Trans. Syst. Man Cybern.*, **54** (2024), 2626–2637. https://doi.org/10.1109/TSMC.2023.3341847

32. Y. B. Wu, T. Wu, J. Liu, L. Xue, Dynamic event-triggered fixed-time synchronization of multi-layer complex networks under denial-of-service attacks, *Nonlinear Dyn.*, **113** (2025), 16821–16835. https://doi.org/10.1007/s11071-025-11034-1

33. X. Hu, L. Wang, F. Song, C. K. Zhang, Y. He, A practical fixed-time intermittent event-triggered control scheme for complex dynamical networks, *IEEE Trans. Syst. Man Cybern.*, **441** (2023), 127618. https://doi.org/10.1109/TSMC.2025.3649923

34. F. Radicchi, A. Arenas, Abrupt transition in the structural formation of interconnected networks, *Nat. Phys.*, **9** (2013), 717–720. https://doi.org/10.1038/nphys2761

35. C. De Persis, P. Tesi, Input-to-state stabilizing control under denial-of-service, *IEEE Trans. Autom. Control*, **60** (2015), 2930–2944. https://doi.org/10.1109/TAC.2015.2416924

36. S. Feng, P. Tesi, Resilient control under denial-of-service: robust design, *Automatica*, **79** (2017), 42–51. https://doi.org/10.1016/j.automatica.2017.01.031

37. G. H. Hardy, J. E. Littlewood, G. Polya, *Inequalities*, Cambridge University Press, 1934.

38. K. H. Johansson, M. Egerstedt, J. Lygeros, S. Sastry, On the regularization of Zeno hybrid automata, *Syst. Control Lett.*, **38** (1999), 141–150. https://doi.org/10.1016/S0167-6911(99)00059-6

39. W. P. M. H. Heemels, K. H. Johansson, P. Tabuada, An introduction to event-triggered and self-triggered control, *Proceedings of the 51st IEEE Conference on Decision and Control*, 2012, 3270–3285. https://doi.org/10.1109/CDC.2012.6425820

AIMS Press